

Received February 27, 2021, accepted March 11, 2021, date of publication March 24, 2021, date of current version August 13, 2021.

Digital Object Identifier 10.1109/ACCESS.2021.3066654

Assessment of Thermal Aging Degree of 10kV Cross-Linked Polyethylene Cable Based on Depolarization Current

YI-YI ZHANG¹, (Member, IEEE), FENG-YU JIANG^{1,2}, XIAO-YONG YU³, KE ZHOU³, WEI ZHANG³, QIANG FU⁴, AND JIAN HAO⁵

¹Guangxi Key Laboratory of Power System Optimization and Energy Technology, Guangxi University, Nanning 530004, China

²College of Electrical Engineering, Zhengzhou University, Zhengzhou 450000, China

³Guangxi Electric Power Research Institute, Nanning 530000, China

⁴Electric Power Research Institute, China Southern Power Grid Company Ltd., Guangzhou 510080, China

⁵State Key Laboratory of Power Transmission and Distribution Equipment, Chongqing University, Chongqing 400044, China

Corresponding author: Yi-Yi Zhang (yiyizhang@gxu.edu.cn)

This work was supported in part by the National Natural Science Foundation of China under Grant 51867003, in part by the Natural Science Foundation of Guangxi under Grant 2018JJB160064 and Grant 2018JJA160176, in part by the Guangxi Bagui Young Scholars Special Funding, in part by the Boshike Award Scheme for Young Innovative Talents, in part by the Guangxi Key Laboratory of Power System Optimization and Energy Technology Project under Grant AE3020001829, in part by the Guangxi Science and Technology Base and Talent Special Project under Grant 2019AC20096, and in part by the Basic Ability Improvement Project for Young and Middle-aged Teachers in Universities of Guangxi under Grant 20190067 and Grant 20190046.

ABSTRACT During the long-term operation of high-voltage cross-linked polyethylene (XLPE) cables, the cable will gradually deteriorate under the effect of various aging factors. Thermal aging is one of the key factors directly related to the long-term operation reliability of the XLPE cables. In this paper, the thermal aging samples are prepared for PDC measurement. Based on the polymer trap theory and the extended Debye model, the shape of PDC curve, depolarization charge, parameters of the extended Debye model, aging factor (A), elongation at break retention rate (EB%) and their relationships under different thermal aging degrees are analyzed. The results show that the depolarization current curve and the depolarization charge can preliminarily judge the aging condition of the XLPE, but it is not accurate enough. R_3 and τ_3 of the branch, with the largest time constant must be the most sensitive to cable aging. With the increase of aging degree, the A shows an upward trend, and has a nonlinear relationship with EB%. Under the aging temperature of 140 °C, after 15-25 days of aging, the A suggests the samples are in the moderate to severe aging stage, and the PDC test should be performed on carried out for the cables with that have been used for 21 years of operation to evaluate the insulation aging condition. The study reveals that the PDC-based parameters can be serviced as an effective tool for the aging condition prediction of XLPE cable insulation.

INDEX TERMS XLPE cable, polarization/depolarization current (PDC), thermal aging, insulation diagnosis, aging factor, elongation at break.

I. INTRODUCTION

Nowadays, XLPE power cable has been used more and more widely [1], [2]. As the most important equipment for energy transmission in the power grid, the XLPE cable will cause unpredictable losses to the national economy once it fails. Its insulation capacity is mainly determined by the XLPE insulation layer, which can directly affect the stability and life of the cable. Existing researches have indicated that long-term exposure of the power cable to high temperature, water

and electric field for a long time that will cause insulation problem [3], [4]. Among them, thermal aging is key factor for insulation performance [5]. According to IEC-60502, during operation, the maximum temperature of cable insulation can reach 90 °C, even up to 250 °C when faults occur. The thermal aging caused by cable overheating will bring irreversible damage to the XLPE insulation, and the high temperature will promote the formation of water trees and electricity tree to a certain extent, which leads to the decline of cable insulation performance eventually [6]–[8]. The degradation of the insulation capacity will reduce the reliability of power transmission and even affect the safe operation of the power grid.

The associate editor coordinating the review of this manuscript and approving it for publication was Mira Naftaly.

Therefore, it is necessary to assess the insulation performance of XLPE cables going through thermal aging.

To detect the cable insulation condition, the commonly used methods include 50Hz dielectric loss, leakage current, partial discharge, etc [9]–[11]. These methods have been widely recognized in actual cable detection, but there are still shortcomings. For example, 50Hz dielectric loss is not very sensitive to aging characterization, and its anti-interference capability is poor. The information of insulation resistance and leakage current is limited, which cannot comprehensively evaluate the insulation condition of the cable. The partial discharge has achieved remarkable achievements in the detection of local defects of the cable, but it is easily affected by external factors and has a high detection error rate. In recent years, the polarization/depolarization current (PDC) method based on the dielectric response principle has been gradually recognized by scholars and used in the condition diagnosis of high voltage electrical equipment, with its advantages of using light equipment, short test time, and reflecting sufficient information [12]. It mainly includes the return voltage (RVM) method [13], the polarization/depolarization current (PDC) method [14], [15], and the frequency domain spectroscopy (FDS) method [16]–[21]. They have been widely used in the analysis and detection of the insulation condition of the oil paper insulated transformer. Whereas, few relevant researches focus on cables. The reason is that according to the actual situation of projects, the RVM method is greatly affected by the length of cables, while the FDS method requires a large capacity of the power supply, which largely limits the application of these two methods in the XLPE cables. Only the PDC method based on time domain dielectric response technology is more suitable for cables, because the measurement using the PDC method is convenient and intuitive results can be obtained [22].

Leibfried T *et al.* proposed that the PDC method can detect insulating materials in time domain. As long as the time is long enough, the PDC method can reflect rich dielectric information [23]. The dielectric information of PDC curve (e.g., slope and shape) are considered, which can effectively reflect the aging condition of insulation [22], [24]. However, the length and structure of cables affect the amplitude and shape of the PDC curve [23]. Gang Ye *et al.* studied how to characterize the severity of the XLPE water tree aging by the PDC method [25]. Based on a large number of experiments, Peter B *et al.* pointed out that aging factor A is not affected by the cable length, the polarization voltage, and the polarization time. Cables can be evaluated by four aging grades: good, middle aging, obvious aging, and serious aging [26]. It provides a reference for the analysis of the thermal aging state. In summary, considering the field operation of cables, methods that include making water tree aging or electrical aging samples are mainly used in studies. In comparison, few studies focus on the diagnostic method of the PDC under the cumulative effect of thermal aging. As a world recognized standard, the elongation at break characterizing mechanical properties is closely related to thermal aging. Referring to

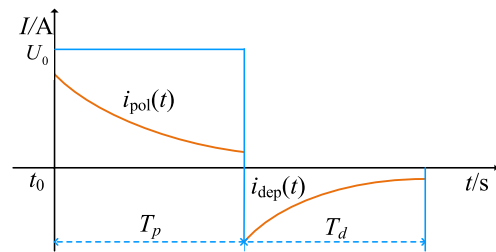


FIGURE 1. Principle of polarization/depolarization current measurement.

ICE 60076, when EB% = 50%, the XLPE cable has reached its end of life and should be decommissioned. However, the relationship between EB% and insulation condition has not been fully analyzed. Therefore, how to use the PDC method to accurately analyze and diagnose the insulation condition of thermal aging cable is an urgent task.

In this study, the research object is 10kV XLPE cable. To diagnose the insulation condition of the XLPE cables with different thermal aging degrees, the artificial accelerated thermal aging experiment at 140 °C of XLPE is carried out, and a high voltage time domain dielectric response test platform is built for the first time. Based on this platform, the polarization/depolarization current variation of 10kV XLPE cables is tested and analyzed. Subsequently, based on the polymer trap theory and the extended Debye model, the equivalent model parameters are calculated, and the aging factor is obtained by introducing the third-order exponential decay method. Besides, the elongation at break that is greatly affected by thermal aging is discussed.

II. THEORETICAL BASIS

A. PRINCIPLE OF PDC METHOD

The polarization depolarization current reflects the slow polarization process of the medium, and the measurement process is shown in Fig. 1 [27]. When a DC step voltage U_0 is applied to a fully discharged uniform dielectric, the current flowing through the dielectric is called the polarization current. The current consists of three parts: conduction current, instantaneous charging current caused by displacement polarization, and absorption current caused by relaxation polarization. The expression is as follows [28]:

$$i_{\text{pol}}(t) = C_0 U_0 \left[\frac{\sigma_0}{\varepsilon_0} + \varepsilon_\infty \delta(t) + f(t) \right] \quad (1)$$

where, U_0 is the geometric capacitance of the dielectric to be measured, σ_0 is the DC conductivity of the dielectric, ε_0 is the vacuum dielectric constant, ε_∞ is the optical frequency dielectric constant of the dielectric, t is the measurement time, $\delta(t)$ is the Dirac function, which exists only at the time of pressure and is infinite, $f(t)$ is the dielectric response function.

After charging for a period of time, the external voltage U_0 is cancelled, and the two ends of the medium are short circuited. At this time, the current flowing through the medium is called the depolarization current. The direction

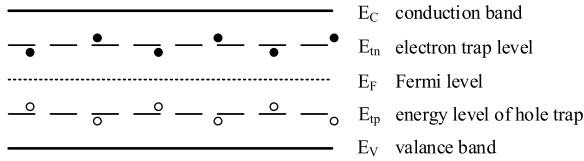


FIGURE 2. Carrier level distribution of trapped traps.

of depolarization current is opposite to that of polarization current, which is only caused by instantaneous displacement polarization and relaxation polarization. According to the superposition principle, the depolarization current $i_{dep}(t)$ is expressed as:

$$i_{dep}(t) = -C_0 U_0 [f(t) - f(t + T_p)] \quad (2)$$

where, T_p is the dielectric continuous charging time.

The XLPE insulation layer contains impurities and defects, forming different trap energy levels. According to the theory of Simmons and Tam [29], trap energy levels in polymer are distributed in the whole energy level range. The electron trap level above the Fermi level mainly contains electrons, while the hole trap energy level below Fermi level mainly contains holes. The electron Fermi distribution function and the hole Fermi distribution function are symmetrical about Fermi level. Therefore, the distribution of trap energy level density in polymer can be characterized just by analyzing the region above the Fermi level occupied by electrons. The energy level distribution of trapped charge carriers is shown in Fig. 2.

During the process of polarization, the charge filled in the defect will transition, and the hot electron will escape from the XLPE. Only the trap region above the Fermi level needs to be considered. The relationship between energy of electron trap E_T and time t can be expressed as follows [30], [31]:

$$E_T(t) = |E_c - E_m| = Kt \cdot \ln(vt) \quad (3)$$

where, $|E_c - E_m|$ is electron trap energy level, K is the Boltzmann constant, v is electron vibration frequency. In addition, the isothermal decay relationship between depolarization current and time in the XLPE can be expressed as [24]:

$$i_{dep}(t) = \frac{qdKT}{2t} f_0(w) \cdot N(E) \quad (4)$$

where $f_0(w)$ is initial density of electron trap, $N(E)$ is the density of trap energy level, q is charge of the electron, d is the thickness of insulation. Obviously, $i_{dep}(t)t$ is directly proportional to $N(E)$, and $i_{dep}(t)$ can be used to study the density of electron trap energy level in insulating materials.

B. EXTENDED DEBYE MODEL

The relaxation process of any dielectric can be represented by both energy dissipation or storage elements, such as the extended Debye model [32], [33]. In the extended Debye model, it is assumed that a certain dipole group is randomly distributed in the whole insulation and changes evenly over time. It is an important premise that the model can represent

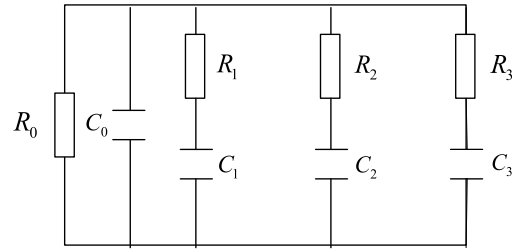


FIGURE 3. Extend Debye model.

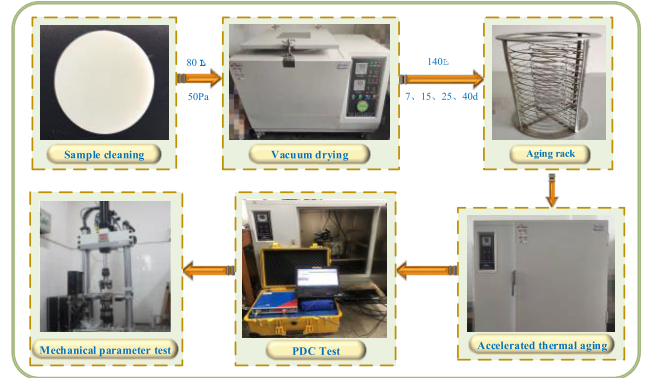


FIGURE 4. Experimental flow chart.

the relaxation process of a specific dipole group with a single RC branch in series.

When the temperature of the process shown in Fig. 1 is constant, the charge transferred out of the medium appears as a short-circuit current in the external circuit. The size of short-circuit current represents the density of defects in the medium, and the change of short-circuit current over time represents the depth of traps in the medium. For the XLPE, the polarization process can be divided into three main processes: the subject polarization process, the polarization process of amorphous and crystal interface, and the interface polarization of metal salts and hydrated ions caused by aging. Therefore, the series connection of capacitance and resistance can be used to represent a specific polarization type. As shown in Fig. 3, the three branches of the extended Debye model are connected in series with resistors and capacitors, representing the above three different polarization processes [32].

III. EXPERIMENTAL DESIGN

A. PRETREATMENT OF XLPE SAMPLES

The insulation performance of cable is determined by the insulation layer. In this paper, the XLPE discs are used to represent cable insulation for research so as to process samples conveniently for measuring parameters. The overall experimental process is shown in Fig. 4.

The disk samples are processed from 10kV XLPE material produced by Nordic Chemical Company, with a thickness of $1.5(\pm 0.05)$ mm and a radius of $16(\pm 0.2)$ cm. Fig. 5 shows the structure of a sample. The samples are cleaned with

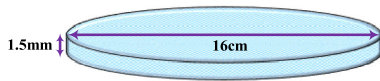


FIGURE 5. XLPE disc sample.

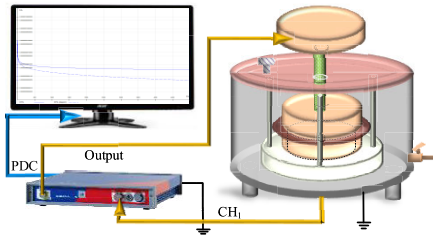


FIGURE 6. Wiring diagram for dielectric response test.

anhydrous ethanol to remove the impurity pollution on the surface, and then placed in a vacuum drying oven for 48h at 80 °C and 50pA to eliminate the influence of water vapor, crosslinking by-products and mechanical stress.

B. PREPARATION OF THERMAL AGING SAMPLES

Thermal aging can destroy the crystallization of insulating materials. For a long time, crystal separation will occur in the XLPE, and the aging effect is obvious. In this paper, the various aging degree of the XLPE samples are achieved by accelerating thermal aging at 140°C, and the aging time are 7days, 15 days, 25 days and 40 days (Fig. 4).

C. PDC TEST OF AGED SAMPLES

In order to improve the stability of measurement data, the three-electrode dielectric response measurement device is designed. The experiment is carried out at 60°C, and samples in section 3.2 are placed in the three-electrode to obtain the PDC curves. The $i_{pol}(t)$ and $i_{dep}(t)$ are measured by DIRANA with 200V (polarization voltage) and 1500s (polarization depolarization time). The PDC measurement wiring is shown in Fig. 6. Since the current is easily disturbed during the measurement process, the three-electrode must be placed in the metal shielding box and grounded to reduce the influence of external electromagnetic interference on measurements.

IV. RESULTS AND DISCUSSION

A. PDC TEST RESULTS OF XLPE

The polarization/depolarization current of the XLPE sample can be recorded in the experiment, but the polarization current is greatly affected by the voltage stability, frequency stability, harmonics and other factors. In addition, the polarization current curve value tends to the volume conductance current of the XLPE layer, which makes the data analysis more complicated, while the depolarization current does not include the conductance current. Thus, the depolarization current is used in this study to judge the XLPE aging degree. Fig. 7 shows curves of the depolarization current of samples. Since switching power supply may lead to the impulse current, curves discussed in this paper are obtained after 10s.

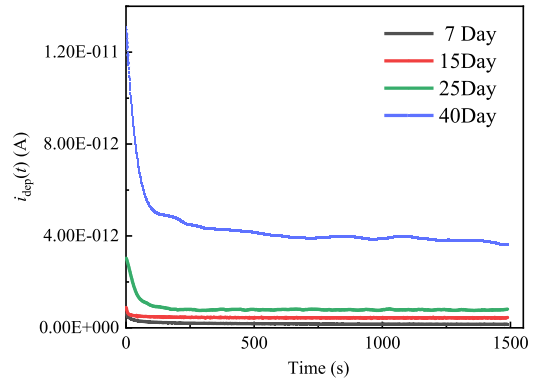


FIGURE 7. Depolarization current of XLPE with different aging time.

In Fig. 7, the amplitude of the sample current is at pA level. Current is divided into two parts roughly. The current in the front part (i.e., high-frequency part) decreases rapidly, while that in the middle and rear part (i.e., low-frequency part) stabilizes gradually. In addition, with the increase of aging time, the critical point of the two parts gradually moves to the left, and the current value becomes larger when it is relatively stable. For example, the depolarization current of samples aged for 7 days needs a period of time to reach the steady value, while the depolarization current of samples aged for 25 and 40 days only takes tens of seconds. That is because thermal aging can increase the number of defects in the XLPE and destroy the cross-linked structure, resulting in more aging products, charged particles and molecular groups. These accelerate the discharge process and increase the conductivity.

B. INFLUENCE OF THERMAL AGING ON DEPOLARIZATION CHARGE AND PARAMETERS OF EXTENDED DEBYE MODEL

1) VARIATION OF DEPOLARIZATION CHARGE

With the increase of aging time, the defects in the cable insulation layer increase, which makes the ability of XLPE to capture space charge become stronger. Therefore, if only the level above the Fermi is considered, the discharge current $i_{dep}(t)$ will increase with the aging time. The depolarization current has been divided into two parts in section 4.1. The discharge quantity of two parts is directly affected by the aging degree. The discharge capacity of the two parts can be calculated by equation (5), and the change with aging time is shown in Fig. 8.

$$\begin{cases} Q_1 = \int_{60}^{1490} i_{dep}(t)dt \\ Q_2 = \int_1^{60} i_{dep}(t)dt \end{cases} \quad (5)$$

It can be seen from Fig. 8 that Q_1 and Q_2 increase with aging time. The relationship between Q_1 and aging time is shown in equation (6), and the relationship between Q_2 and t is shown in equation (7). Q_1 is more sensitive to the aging degree, so the low frequency discharge of depolarization

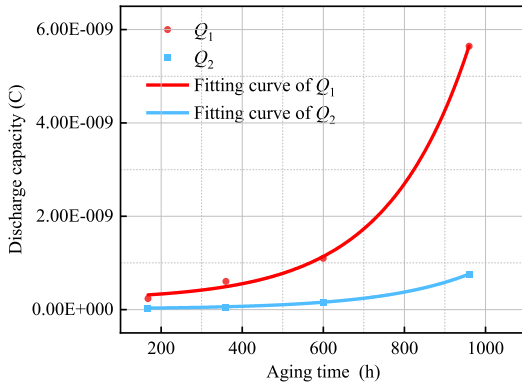


FIGURE 8. Relationship between discharge quantity and aging time.

current can well reflect the aging degree of the XLPE.

$$Q_1 = 4.96 \times 10^{-11} \exp\left(\frac{t}{204.34}\right) + 1.99 \times 10^{-10} \quad (6)$$

$$Q_2 = 9.80 \times 10^{-12} \exp\left(\frac{t}{221.27}\right) + 7.41 \times 10^{-12} \quad (7)$$

2) PARAMETER CHARACTERISTICS OF THE EXTENDED DEBYE MODEL

In the extended Debye model, R_j and C_j of each branch are used to simulate different relaxation polarization processes of XLPE. The number of polarization types determines the number of branches [34]. There are three types of polarization process in the XLPE, and their equivalent circuit models are shown in Fig. 3. If the time constant $\tau_j = R_j C_j$, the depolarization current fits into the equation (8) and equation (9) [33], [35]:

$$i_{dep}(t) = \sum_{j=1}^3 \alpha_j e^{-\frac{t}{\tau_j}} \quad (8)$$

where, α_j and τ_j are related to the characteristics of dielectric material. α_j reflects the density of trap, and τ_j reflects the depth of trap. j represents three polarization types. $j = 1$ represents the subject polarization of insulation material, $j = 2$ represents the interfacial polarization between crystalline and amorphous states, and $j = 3$ represents the interfacial polarization between various ions and groups after aging. α_j is a coefficient, τ_j is time constant.

$$\alpha_j = U_0 \frac{1 - e^{-\frac{t}{\tau_j}}}{R_j} \quad (9)$$

The end of the depolarization current curve mainly depends on the resistance and capacitance of j -max branch [32]. According to this principle, parameters of branch $j = 3$ can be obtained by fitting the end of $i_{dep}(t)$ with equation (8). Subtracting the current generated by branch $j = 3$ from $i_{dep}(t)$, the end of the residual current curve is used to fit branch $j = 2$. By analogy, the parameters of each branch of the equivalent circuit can be determined, and the calculation results are shown in Table 1.

In Table 1, R and τ of each branch gradually decrease with the increase of aging time, and $R_3 > R_2 > R_1$, $\tau_3 > \tau_2 > \tau_1$.

TABLE 1. Main parameters of the extended Debye model for samples with different aging time.

Aging time (day)	τ_1 (s)	τ_2 (s)	τ_3 (s)	R_1 (Ω)	R_2 (Ω)	R_3 (Ω)
7	15.8	142.1	2837	1.24E+12	2.51E+12	7.73E+12
15	13.7	115.4	2456	9.78E+11	1.42E+12	6.46E+12
25	9.6	86.7	1835	5.66E+11	8.82E+11	4.13E+12
40	5.8	44.3	1179	2.01E+11	5.38E+11	1.87E+12

R_3 is much larger than R_1 and R_2 . This is because branch $j = 1$ and $j = 2$ simulate subject polarization and interface polarization between crystal and amorphous respectively, which are greatly affected by the insulation material and have little correlation with aging degree, especially for branch $j = 1$. However, during the operation of cables, temperature, water-ions and other factors interact with the XLPE for a long time, which will affect the number and type of crystal and aging products. Therefore, the branch $j = 3$ reflecting the interfacial polarization between various ions and groups is greatly affected by aging time. Thermal aging will greatly aggravate the degree of polarization, increasing of the time constant and equivalent resistance of the branch. In addition, the influence of aging on τ_1 is the least, followed by that on τ_2 , while that on τ_3 is the most obvious. It is indicated that τ_2 and τ_3 can reflect the thermal aging degree of the XLPE to some extent. In general, the parameters of branch $j = 2$ and $j = 3$ can provide a reference for the thermal aging condition evaluation of the XLPE.

C. QUANTITATIVE ANALYSIS BY AGING FACTOR A

Through the above analysis, in addition to the subject polarization, the two polarization types and depolarization charge are also sensitive to the aging degree of the XLPE. In order to characterize the insulation aging degree of cable more accurately, the aging factor A is defined. The aging factor is related to the depolarization quantity corresponding to the two polarization types. The expression of aging factor A is as follows:

$$A = \frac{Q(\tau_3)}{Q(\tau_2)} \quad (10)$$

where,

$$\begin{cases} Q(\tau_3) \approx \alpha_1 \tau_1 + \alpha_2 \tau_2 (1 - e^{-\frac{\tau_3}{\tau_2}}) + \alpha_3 \tau_3 (1 - e^{-1}) \\ Q(\tau_2) \approx \alpha_1 \tau_1 + \alpha_2 \tau_2 (1 - e^{-1}) + \alpha_3 \tau_3 (1 - e^{-\frac{\tau_3}{\tau_2}}) \end{cases} \quad (11)$$

The aging factor A of the XLPE at different aging times is given in Table 1. It can be noted that A increases with aging, and the rate of changes gradually decreases. It shows that the insulation performance of cable changes rapidly in the early and middle stage, but that changes slowly in the final stage. This is because the essence of the XLPE thermal aging is the oxidation aging inside the material, which determines the thermal aging characteristics of the XLPE.

TABLE 2. The value of A at different aging time.

Aging time	7days	15days	25days	40days
A	1.56	1.69	2.03	2.38

TABLE 3. Aging factor for evaluating XLPE insulation condition.

A	<1.75	1.75~1.90	1.90~2.10	>2.10
Insulation performance	Good	Moderate aging	Severe aging	Retire

In the oxidation process, a series of physical and chemical reactions need reactants, but reactants are limited. With the increase of aging time, the concentration of reactants will decrease, resulting in a slow degradation rate. In addition, in the later stage of thermal aging, physical aging gradually dominates caused by the decrease of chemical reactions, though physical aging is slow at a certain temperature. Finally, the difference of A decreases in the later stage of the XLPE aging.

Table 3 shows the aging factor evaluation standard with high international recognition. Comparing the value of four samples, it can be inferred that the XLPE is in the good insulation stage when the aging time is 7 days and 15 days. When the aging time is 25 days, it is in the severe aging stage. Referring to IEC-60076, when the insulation temperature exceeds the allowable temperature, the aging rate will double for every 6 °C increase. Therefore, the sample aged 25 days is equivalent to the cable used for 21 years. When the aging time is 40 days, the sample is in the severe aging stage, and the cables with the corresponding operation time should be considered for decommissioning.

D. MECHANICAL PARAMETERS: ELONGATION AT BREAK

The mechanical properties of polymers are related to its molecular weight, molecular polarity, situation of crosslinking and crystallization, and defects in polymers. During the thermal aging process of the XLPE, the thermal cracking and thermal oxygen cracking reaction will cause the fracture of polymer chain and the destruction of the whole crosslinking network. Consequently, the thermal aging of cables will not only reduce the insulation capacity, but also cause material cracks, deformation and other phenomena, reducing the mechanical properties of cables.

The elongation at break can reflect the mechanical aging degree of the XLPE, and the elongation at break retention EB% is a recognized standard to judge the insulation failure of the XLPE [14]. When EB% = 50%, the insulation performance of cables is lower than the standard of safe operation. EB% can be calculated by equation (12).

$$EB\% = \frac{k}{k_0} \tag{12}$$

where, k_0 is the elongation at break of the unaged sample, k is the elongation at break of the aged sample.

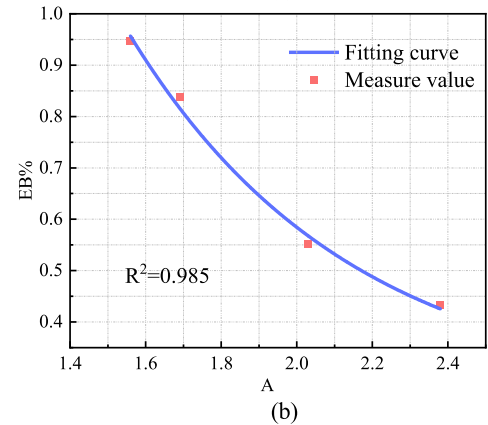
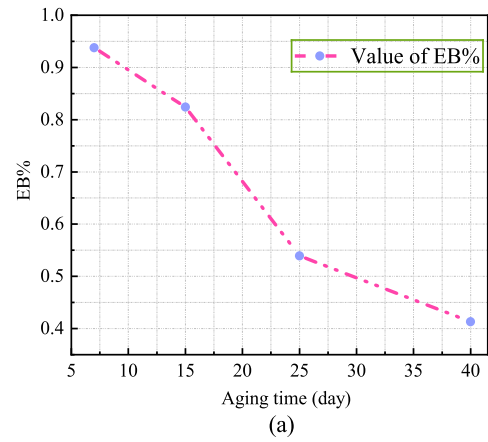


FIGURE 9. Relationship between EB% and aging time and A: (a) Relationship between EB% and aging time, (b) The relationship between A and EB%.

As shown in Fig. 9 (a), EB% decreases with aging time. In particular, the decrease rate of EB% is the highest in the second half of the early aging period and the middle aging period, and that is the lowest in the late aging period. The results show that the mechanical property of the XLPE is negatively correlated with the aging degree, and it decreases most rapidly in the early and middle stages of aging. A and EB% have similar changes in aging, and both of them can provide a reference for evaluating aging conditions. Fig. 9 (b) shows the relationship between the calculated EB% and A.

In Fig. 9 (b), the fitting curve of A and EB% is shown in equation (13). The A and EB% have a good fitting relationship. If the value of the state boundary point in Table 2 is substituted into equation (13), the corresponding elongation at break can be calculated. Meanwhile, from brand new to end of life, EB% of cable drops from 100% to 50%. 0.833 and 0.667 divide EB% into three sections ideally. Fig. 10 shows its relevance. It is not difficult to find that the error between the ideal value and the measured value is small, which shows that there is a corresponding relationship between mechanical characteristic quantity and electrical characteristic quantity.

$$EB\% = 10.07 \times \exp\left(-\frac{A}{0.59}\right) + 0.251 \tag{13}$$

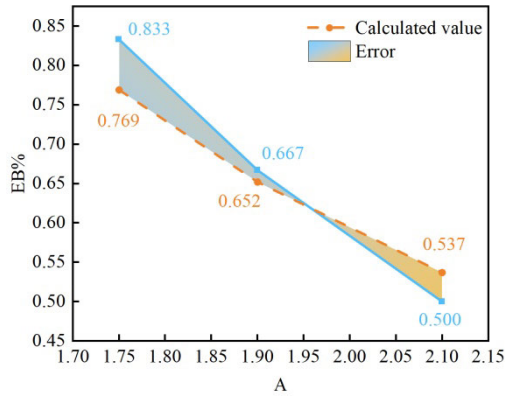


FIGURE 10. Comparison of ideal and calculated value critical point of EB%.

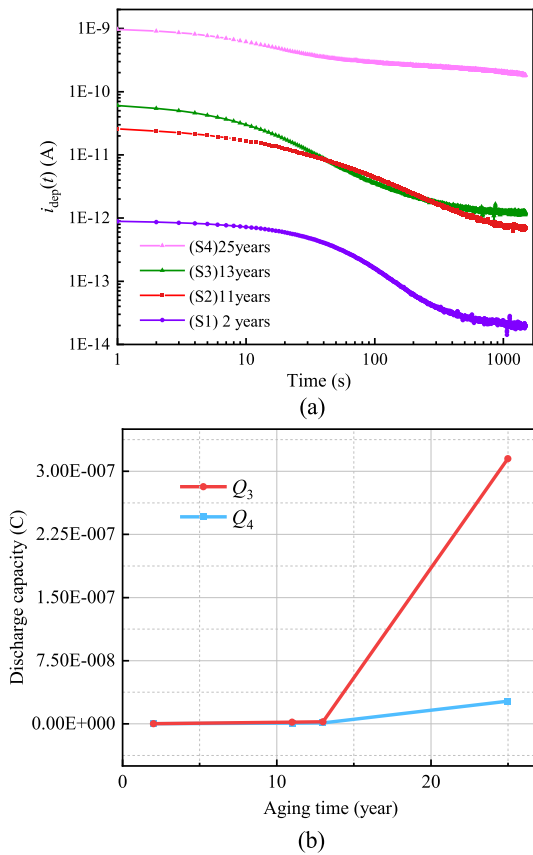


FIGURE 11. The dielectric response test results of 10kV cables in operation: (a) The PDC curve of 10kV cables in operation, (b) Calculation results of low frequency and high frequency discharge of cables.

V. VERIFICATION OF EXPERIMENTAL RESULTS

The premise of the above results is taking the XLPE thermal aging samples prepared in the laboratory as the research object. To verify the feasibility and accuracy of the method, four 10kV XLPE cables in operation are considered as the research object in this section. The depolarization current and discharge capacity are shown in Fig. 11.

In Fig. 11, the PDC curve characteristics of cables with different service life basically conform to the results in section

4.1. The time corresponding to the inflection point of S1, S3 and S4 decrease gradually, and the steady-state current of the four cables conforms to $S1 < S2 < S3 < S4$. Fig. 11 (b) can be obtained by calculating the curve of Fig. 11 (a) using equation (5). With the increase of aging time, the increment of Q_4 is obviously larger than that of Q_3 . The overall trend of low-frequency and high-frequency discharge is consistent with the previous analysis. At the same time, the discharge capacity is affected by the length of the tested cable, test temperature and other factors. Therefore, although equation (6) and equation (7) are not universal, it is still helpful to analyze the depolarization current characteristics and its variation law of the XLPE thermal aging.

Parameters of the extended Debye model of cables are calculated by equation (8), while the aging factor of the four tested cables is calculated by equation (10) and equation (11), as shown in Table 4. If the insulation state of the XLPE is worse, the branch resistance will be larger and the time constant of the extended Debye model will be smaller. As shown in Table 4, R_3 of S4 is obviously larger than that of other cables, and τ_3 is smaller than that of the others. By comparing the equivalent resistance and time constant of each branch of cables with different service life, it can be concluded that R_3 is more sensitive to the aging state of cables, which is consistent with the previous analysis. Besides, the aging factor increases with the aging time. According to Table 2, S1 has just entered the early aging stage and has an excellent insulation performance. For S2 and S3 in middle life, the S2 is about to enter the late aging stage, while the S3 is already serious aging. Although there is no significant difference in their service life, the A of them are significantly different. The result shows that the aging rate of the XLPE is larger in the middle of its life, so the insulation condition detection of cables used more than 13 years should be strengthened appropriately, especially after 21 years. Furthermore, as the only decommissioned cable, the A of S4 is 2.13, which is larger than 2.1, so it should be decommissioned theoretically. The result is consistent with reality. In conclusion, it is accurate and feasible to analyze and evaluate the thermal aging condition of the XLPE cable by aging factor, which can provide a reference for the operation and maintenance of the power system.

Finally, four cables were sliced, and their elongation at break was tested. The initial elongation at break refers to the data provided by the manufacturer. Fig. 12 shows the value of EB%. The decline rate of EB% of real cable in the early and middle stage is significantly higher than that in other stages. Furthermore, using the obtained aging factor and equation (13), the value of EB% can be calculated. Fig. 12 (b) compares the calculated and measured values. In comparison, the error between the calculated value and the measured value is very small.

According to the above analysis, although the depolarized high-frequency and low-frequency electric quantity of the XLPE cable is affected by the experimental conditions and cable size, it cannot be quantitatively evaluated, but it still

TABLE 4. Parameters of the extended Debye model and aging factors of four real cables.

Number	τ_1 (s)	τ_2 (s)	τ_3 (s)	R_1 (Ω)	R_2 (Ω)	R_3 (Ω)	A
S1	9.3	198.1	3835	1.59E+12	2.77E+12	7.82E+12	1.75
S2	7.1	136.5	2981	7.23E+11	1.34E+12	5.77E+12	1.89
S3	6.8	112.6	2633	6.39E+11	1.03E+12	4.93E+12	1.95
S4	3.8	69.7	1794	3.16E+11	6.12E+11	2.66E+12	2.13

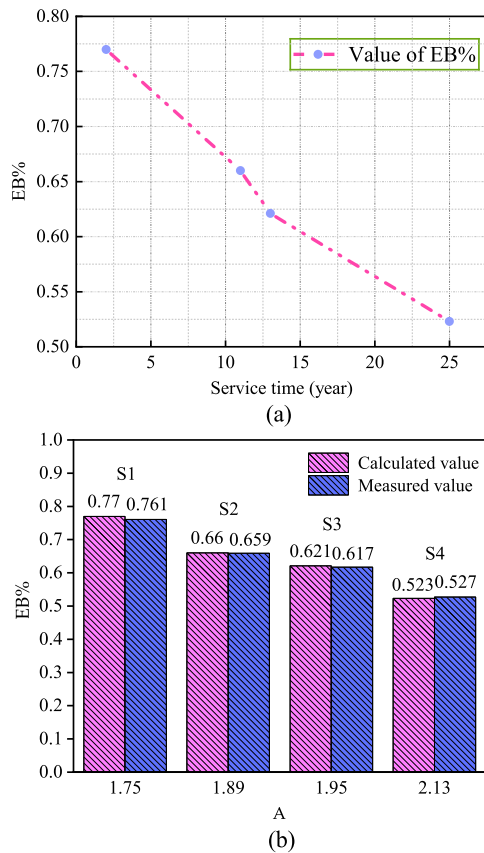


FIGURE 12. The value of EB%: (a) The relationship between the service time of the actual cable and EB%, (b) Comparison of the measured and calculated values of EB% for real cables.

can provide a reference for qualitative analysis. At the same time, the τ and R of the maximum time constant branch in the extended Debye model are closely related to the aging degree, and the A obtained from this premise can characterize the aging condition of the cable effectively. There is a good fitting relationship between A and EB%. The trisection points of EB% (50%~100%) is basically equivalent to A corresponding to the critical point of the insulation state.

VI. CONCLUSION

In this paper, 10kV XLPE is taken as the research object. After samples are prepared by accelerated thermal aging, the PDC test and the elongation at break test are carried out, and the curve, depolarization charge, aging factor and other parameters are analyzed. The following conclusions were obtained:

1) Compared with the existing test methods, the PDC-based method can overcome the shortcomings of the distributed fault diagnosis, such as reflecting less information and having destructiveness. The insulation aging condition of the cable can be judged by the depolarization current attenuation curve. If the aging is more serious, the current in the low frequency part of the curve will be larger and the discharge capacity will be greater.

2) In the extended Debye model of the XLPE, the branch resistance and time constant decrease with the increase of aging time. R_3 and τ_3 of the branch with the largest time constant must be the most sensitive to cable aging.

3) Aging factor A can quantitatively describe the aging degree of the XLPE. It is found that the value of A is positively correlated with the degree of the XLPE thermal aging. Under aging temperature of 140 °C, the samples aged for 25 days are in the serious aging state, and it is equivalent to the cable that has been used for 21 years. In addition, the sample aged for 40 days cannot meet the requirements of normal operation. Therefore, attention should be paid to the diagnosis of the aging state of the XLPE cables with operation time of about 21 years.

4) Through further test of elongation at break, it can be found that A and EB% have a certain nonlinear relationship. Moreover, as the critical value of aging factor, 1.75, 1.90, 2.10 divide cable into four thermal aging stages. The EB% corresponding to the three values can divide EB% into three equal parts basically, from 50%~100%.

REFERENCES

- [1] K. Barber, "Power cables in energy development in the 21st century," in *Proc. IEEE Power Eng. Soc. Winter Meeting Conf.*, vol. 1, Jan. 2000, pp. 564–568.
- [2] T. J. Hammons, "Power cables in the twenty-first century," *Electr. Power Compon. Syst.*, vol. 31, no. 10, pp. 967–994, Oct. 2003.
- [3] E. David, J.-L. Parpal, and J.-P. Crine, "Aging of XLPE cable insulation under combined electrical and mechanical stresses," in *Proc. Conf. Rec. IEEE Int. Symp. Electr. Insul.*, vol. 2, Jun. 1996, pp. 716–719.
- [4] *Country Cooperation Strategy and Saudi Arabia*, World Health Org., Geneva, Switzerland, 2011, pp. 1–14, no. 57.
- [5] D. P. Duan, Y. Zeng, C. J. Huang, G. H. Sheng, X. C. Jiang, and C. X. Sun, "Digital algorithm based on orthogonal decomposition for measurement of dielectric loss factor," *IET Gener. Transmiss. Distrib.*, vol. 2, no. 6, pp. 868–875, 2008.
- [6] A. A. Al-Arainy, A. A. Ahaideb, M. I. Qureshi, and N. H. Malik, "Statistical evaluation of water tree lengths in XLPE cables at different temperatures," *IEEE Trans. Dielectr. Electr. Insul.*, vol. 11, no. 6, pp. 995–1006, Dec. 2004.
- [7] M. Nedjar, A. Bérroual, and A. Boubakeur, "Influence of thermal aging on the electrical properties of poly(vinyl chloride)," *J. Appl. Polym. Sci.*, vol. 102, no. 5, pp. 4728–4733, 2006.

- [8] A. Maruyama, F. Komori, Y. Suzuoki, T. Okamoto, and T. Nagata, "High temperature PD degradation characteristics in bulk and interfaces of insulating materials for power cables," in *Proc. IEEE Int. Conf. Properties Appl. Dielectr. Mater.*, vol. 1, Jun. 2000, pp. 264–267.
- [9] L. Chmura, P. Cichecki, E. Gulski, J. J. Smit, and F. De Vries, "Life time estimation of serviced aged oil-paper insulated HV power cables based on the dielectric loss measurements ($\tan \delta$)," in *Proc. Conf. Rec. IEEE Int. Symp. Electr. Insul.*, Jun. 2010, pp. 1–4.
- [10] H. Ghorbani, M. Saltzer, and C.-O. Olsson, "Observation of non-monotonic dependence of leakage current with temperature during thermal cycling," in *Proc. 34th Electr. Insul. Conf. (EIC)*, Jun. 2016, pp. 488–491.
- [11] D. Fynes-Clinton and C. Nyamupangedu, "Partial discharge characterization of cross-linked polyethylene medium voltage power cable termination defects at very low frequency (0.1 Hz) and power frequency test voltages," *IEEE Elect. Insul. Mag.*, vol. 32, no. 4, pp. 15–23, Jul. 2016.
- [12] T. Šarac, J. Devaux, N. Quiévy, A. Gusarov, and M. J. Konstantinović, "The correlation between elongation at break and thermal decomposition of aged EPDM cable polymer," *Radiat. Phys. Chem.*, vol. 132, pp. 8–12, Mar. 2017.
- [13] R. Patsch, "Return voltage measurements—A promising tool for the diagnosis of the insulation condition of power transformers," in *Proc. IEEE Int. Conf. High Voltage Eng. Appl. (ICHVE)*, Sep. 2018, p. 3.
- [14] J. Liu, H. Zheng, Y. Zhang, T. Zhou, J. Zhao, J. Li, J. Liu, and J. Li, "Comparative investigation on the performance of modified system poles and traditional system poles obtained from PDC data for diagnosing the ageing condition of transformer polymer insulation materials," *Polymers*, vol. 10, no. 2, p. 191, Feb. 2018.
- [15] H. Zheng, B. Lai, Y. Zhang, J. Liu, and S. Yang, "Correction for polarization current curve of polymer insulation materials in transformers considering the temperature and moisture effects," *Polymers*, vol. 12, no. 1, p. 143, Jan. 2020.
- [16] J. Liu, S. Yang, Y. Zhang, H. Zheng, Z. Shi, and C. Zhang, "A modified X-model of the oil-impregnated bushing including non-uniform thermal aging of cellulose insulation," *Cellulose*, vol. 27, no. 8, pp. 4525–4538, May 2020.
- [17] J. Liu, X. Fan, Y. Zhang, H. Zheng, and M. Zhu, "Quantitative evaluation for moisture content of cellulose insulation material in paper/oil system based on frequency dielectric modulus technique," *Cellulose*, vol. 27, no. 4, pp. 2343–2356, Mar. 2020.
- [18] J. Liu, X. Fan, Y. Zhang, C. Zhang, and Z. Wang, "Aging evaluation and moisture prediction of oil-immersed cellulose insulation in field transformer using frequency domain spectroscopy and aging kinetics model," *Cellulose*, vol. 27, no. 12, pp. 7175–7189, Aug. 2020.
- [19] J. Liu, X. Fan, Y. Zhang, S. Li, and J. Jiao, "Frequency domain spectroscopy prediction of oil-immersed cellulose insulation under diverse temperature and moisture," *IEEE Trans. Dielectr. Electr. Insul.*, vol. 27, no. 6, pp. 1820–1828, Dec. 2020.
- [20] J. Liu, X. Fan, Y. Zhang, H. Zheng, and J. Jiao, "Temperature correction to dielectric modulus and activation energy prediction of oil-immersed cellulose insulation," *IEEE Trans. Dielectr. Electr. Insul.*, vol. 27, no. 3, pp. 956–963, Jun. 2020.
- [21] J. Liu, X. Fan, Y. Zhang, H. Zheng, and C. Zhang, "Condition prediction for oil-immersed cellulose insulation in field transformer using fitting fingerprint database," *IEEE Trans. Dielectr. Electr. Insul.*, vol. 27, no. 1, pp. 279–287, Feb. 2020.
- [22] B. S. Oyegoke, "Improved condition assessment of XLPE insulated cables using the isothermal relaxation current technique," in *Proc. Annu. Rep. Conf. Electr. Insul. Dielectr. Phenomena (CEIDP)*, Oct. 2006, pp. 477–480.
- [23] T. Leibfried and A. J. Kachler, "Insulation diagnostics on power transformers using the polarisation and depolarisation current (PDC) analysis," in *Proc. Conf. Rec. IEEE Int. Symp. Electr. Insul.*, Apr. 2002, pp. 170–173.
- [24] M. Beigert and H.-G. Kranz, "Destruction free ageing diagnosis of power cable insulation using the isothermal relaxation current analysis," in *Proc. IEEE Int. Symp. Electr. Insul.*, Jun. 1994, no. 2, pp. 17–21.
- [25] G. Ye, H. Li, F. Lin, J. Tong, X. Wu, and Z. Huang, "Condition assessment of XLPE insulated cables based on polarization/depolarization current method," *IEEE Trans. Dielectr. Electr. Insul.*, vol. 23, no. 2, pp. 721–729, Apr. 2016.
- [26] P. Birkner, "Field experience with a condition-based maintenance program of 20-kV XLPE distribution system using IRC-analysis," *IEEE Trans. Power Del.*, vol. 19, no. 1, pp. 3–8, Jan. 2004.
- [27] O. E. Igwe, "Cable sizing and its effect on thermal and ampacity values in underground power distribution," Univ. Kentucky, Lexington, KY, USA, 2016.
- [28] T. K. Saha, "Review of time-domain polarization measurements for assessing insulation condition in aged transformers," *IEEE Trans. Power Del.*, vol. 18, no. 4, pp. 1293–1301, Oct. 2003.
- [29] J. G. Simmons and M. C. Tam, "Theory of isothermal currents and the direct determination of trap parameters in semiconductors and insulators containing arbitrary trap distributions," *Phys. Rev. B, Condens. Matter*, vol. 7, no. 8, pp. 3706–3713, Apr. 1973.
- [30] P. K. Watson, F. W. Schmidlin, and R. V. L. Donna, "The trapping of electrons in polystyrene," *IEEE Trans. Electr. Insul.*, vol. 27, no. 4, pp. 680–686, Aug. 1992.
- [31] P. K. Watson, "Transport and trapping of electrons in polymers," in *Proc. Annu. Rep. Conf. Electr. Insul. Dielectr. Phenomena (CEIDP)*, 1995, vol. 2, no. 5, pp. 21–27.
- [32] T. K. Saha, P. Purkait, and F. Müller, "Deriving an equivalent circuit of transformers insulation for understanding the dielectric response measurements," *IEEE Trans. Power Del.*, vol. 20, no. 1, pp. 149–157, Jan. 2005.
- [33] A. Kumar and S. M. Mahajan, "Correlation between time and frequency domain measurements for the insulation diagnosis of current transformers," in *Proc. North Amer. Power Symp. (NAPS)*, Sep. 2010, vol. 1, no. 1, pp. 1–5.
- [34] W. S. Zaengl, "Applications of dielectric spectroscopy in time and frequency domain for HV power equipment," *IEEE Elect. Insul. Mag.*, vol. 19, no. 6, pp. 9–22, Nov. 2003.
- [35] P. R. S. Jota, S. M. Islam, and F. G. Jota, "Modeling the polarization spectrum in composite oil/paper insulation systems," *IEEE Trans. Dielectr. Electr. Insul.*, vol. 6, no. 2, pp. 145–151, Apr. 1999.



YI-YI ZHANG (Member, IEEE) was born in Guangxi, China, in 1986. He received the bachelor's degree in electrical engineering from Guangxi University, Nanning, China, in 2008, and the Ph.D. degree in electrical engineering from Chongqing University, Chongqing, China, in 2014. In 2014, he joined Guangxi University, where he is an Associate Professor with the College of Electrical Engineering. He is the author or coauthor of over 50 articles published in SCI journals. His current research interest includes the intelligent diagnosis for transformers.



FENG-YU JIANG was born in Henan, China, in 1995. He received the bachelor's degree in electrical engineering from Zhengzhou University, Zhengzhou, China, in 2017. He is currently pursuing the M.S. degree with Guangxi University, Nanning, China. His current research interests include insulation diagnosis and condition assessment for XLPE power cable insulation.



XIAO-YONG YU was born in Anhui, China, in 1985. He is currently a Senior Engineer with the Guangxi Electric Power Research Institute. He is mainly involved in distribution network fault analysis and distribution automation.



QIANG FU was born in Heilongjiang, China, in 1972. He is currently a Senior Engineer with the Guangxi Electric Power Research Institute. He is mainly involved in power equipment condition monitoring and evaluation research.



KE ZHOU was born in Hunan, China, in 1979. He is currently a Senior Engineer with the Electric Power Research Institute, China Southern Power Grid Company Limited. He is mainly involved in insulation material testing technology.



WEI ZHANG was born in Anhui, China, in 1983. He is currently a Senior Engineer with the Guangxi Electric Power Research Institute. He is mainly involved in power equipment condition monitoring and evaluation research.



JIAN HAO was born in Hebei, China, in 1984. He is currently an Associate Professor with Chongqing University. His research interest includes the development and application of dielectric materials.

...